Simple and accurate modeling of a six-phase axial flux pmsm for fault tolerant control

A. Abdallah, Franck Betin, Amine Yazidi

International Journal of Electrical Engineering and Technology (IJEET)
Volume 12, Issue 12, December 2021, pp. 1-13, Article ID: IJEET_12_12_001
Available online at https://iaeme.com/Home/issue/IJEET?Volume=12&Issue=12
ISSN Print: 0976-6545 and ISSN Online: 0976-6553
DOI: https://doi.org/10.17605/OSF.IO/XDPMN

SIMPLE AND ACCURATE MODELING OF A SIX-PHASE AXIAL FLUX PMSM FOR FAULT TOLERANT CONTROL

A. Abdallah, F. Betin, A. Yazidi

Laboratory of Innovative Technologies, University of Picardie "Jules Verne",
15 Avenue Francois Mitterrand, France

ABSTRACT

Modeling of multi-phase PMSM has been widely studied in the literature. Nevertheless, the methods applied for this achievement are complex due to the strong need to do an analysis of the magnetic field distribution inside the machine. In addition, mathematical transformations and calculations are required to implement such models. In the proposed study, a new modeling method is proposed based on a very simple theoretical computation approach with high accuracy. Its importance is that the model created will be used to do a fault tolerant control for the machine under study. The methodology is explained and presented first, the model is then simulated using the Matlab/Simulink software and finally validated by experimental tests using various topologies and hazards of electrical networks connected to the machine phases.

Key words: Six-phase PM synchronous machine, Modeling, Electromotive forces computation.

Cite this Article: A. Abdallah, F. Betin, A. Yazidi, Simple and Accurate Modeling of a Six-Phase Axial Flux PMSM for Fault Tolerant Control, *International Journal of Electrical Engineering and Technology (IJEET).* 12(12), 2021, pp. 1-13.
https://iaeme.com/Home/issue/IJEET?Volume=12&Issue=12

1. INTRODUCTION

Nowadays, the modern trends of electric machineries in the field requiring high reliability are the multi-phase electric machines due to the advantages they offer over conventional machines. Among these advantages, multi-phase machines present lower currents in the stator windings which means less stresses on the inverters switches and more capability to use smaller inverters [1], lower torque ripples, lower losses and the capability to operate with one or more phases opened which means higher reliability [2]. A continuous operation and a higher reliability are really important in various applications such as in the military and the aerospace fields, in the electrical vehicles [3] and for the renewable energy generation. Among the various multi-phase machines, the six-phase permanent magnet synchronous machines (PMSM) presents many advantages such as the higher efficiency and power density [4].

The modeling of the machine is a necessary start point in order to do a suitable control of the machine both in healthy and faulty conditions. In [5,6,7], the modeling of such machines has been done by procedures based on complicated mathematical computations which are not suitable in the engineering industry. These procedures are based on a sufficient knowledge of the magnetic field distribution inside the machine that cannot be identified in simple methods.

In [8], Singh modeled a six-phase synchronous generator for the application of renewable energy generation, but the mathematical dq transformation is used to achieve such model. In [9], Pantea modeled a six-phase induction machine using only resistances, inductances, and controlled voltage sources. In this paper, coupling effects between both the stator and the rotor have been taken into account by the computation of stator–rotor mutual inductances. So, one solution to model a PMSM is to replace the rotor part of the induction machine in the model by a circuit equivalent to the permanent magnets, but this method still suffer from computational burdens. In [10], Pantea modeled a six-phase permanent magnet machine using the Finite Elements concept. Although this model demonstrated satisfactory results, the main drawback of this modeling technique is that it is really time consuming.

In this paper, we propose a method to model the PMSM based on the equivalent internal circuit of the machine composed of resistances and inductances, and also of electromotive forces generated by the rotor and calculated in a simple way without a need to the dq transformation which complicates the matrices calculations. Once the model is created and validated, it can replace the machine and it will be used to implement any application for the six-phase PMSM under study.

This paper is organized as follows : Section II describes the PMSM used in our laboratory. Section III presents the computation of electromotive forces (EMFs) created by the rotor magnets as well as the voltages generated on the stator. Section IV determines the fraction or percentage of the linkage flux coupled with the stator windings which is required to model the machine. Section V determines the remaining unknown parameters of the stator windings in the machine. Section VI presents the model assessment and the verification of the accuracy obtained. Finally, Section VII ends by a conclusion and gives some paths for further works.

2. DESCRIPTION OF THE SIX-PHASE AXIAL FLUX PMSM

Fig. 1 represents the configuration of the axial flux PMSM machine used in our laboratory while Fig. 2 depicts the windings arrangement of the machine. The stator is composed of six phases 32 poles, and the permanent magnet rotor is composed of double 32 small identical magnets arranged alternatively between North (N) and South (S) from each side of the stator windings.

A diagram of the stator windings distribution of this machine is shown in Fig. 3. The PMSM is of type N-N where the field lines of the rotor magnets interact with the stator windings as shown in Fig. 4. The electrical and geometrical parameters of the PMSM that we are modeling are presented in tables I and II in appendix.

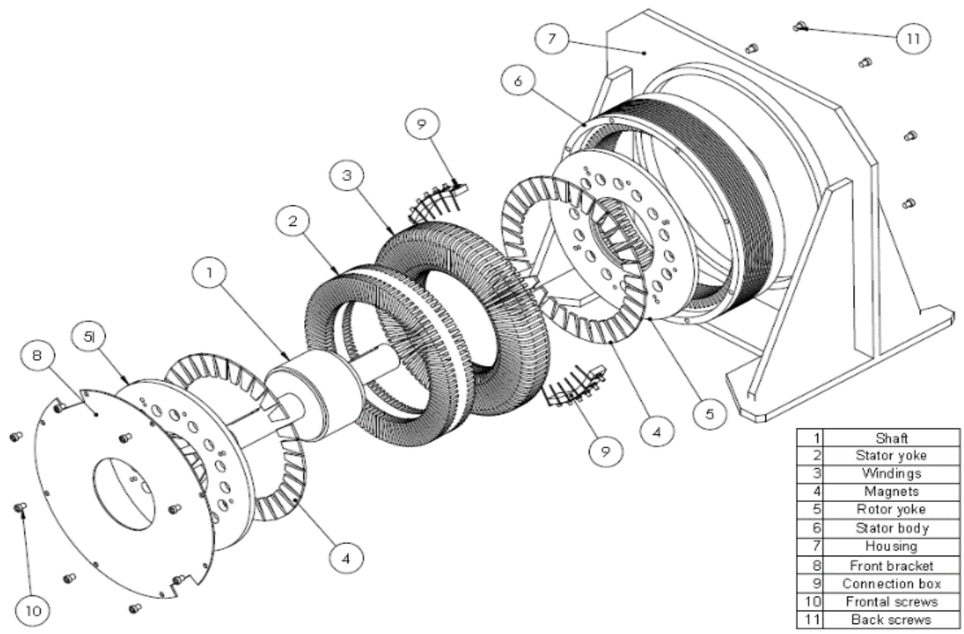

Figure 1 6-phase axial flux PMSM

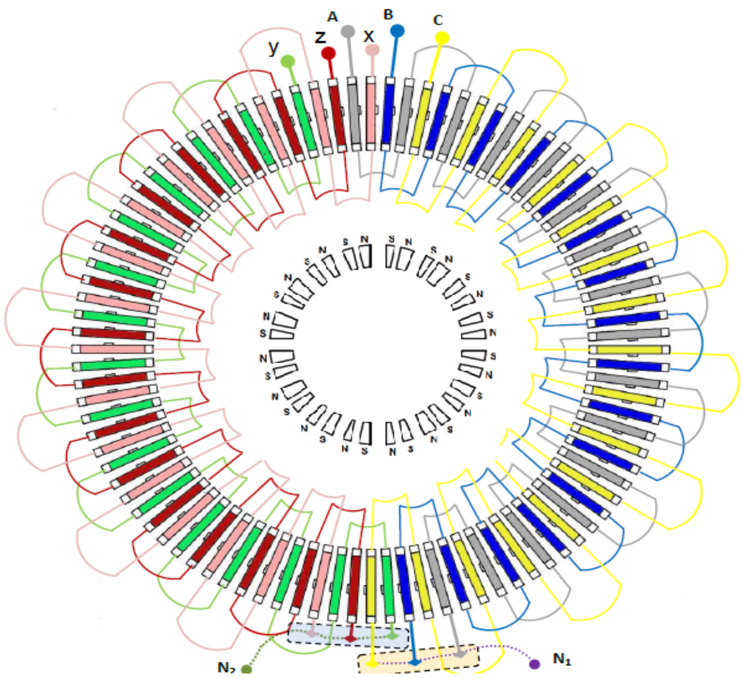

Figure 2 Axial flux PMSM windings arrangement

Since 32 magnets are disposed in a round over 360 degrees, the angle between two adjacent magnets N and S is 11.25 degrees. Furthermore, the machine is a 32 stator poles with 32 rotor permanent magnets, the disposition of the magnet and the pole in a stator phase is the same for all poles. The coils of the poles in each phase are connected in series. Then, the induced flux for the total phase is 32 times the one of a pole.

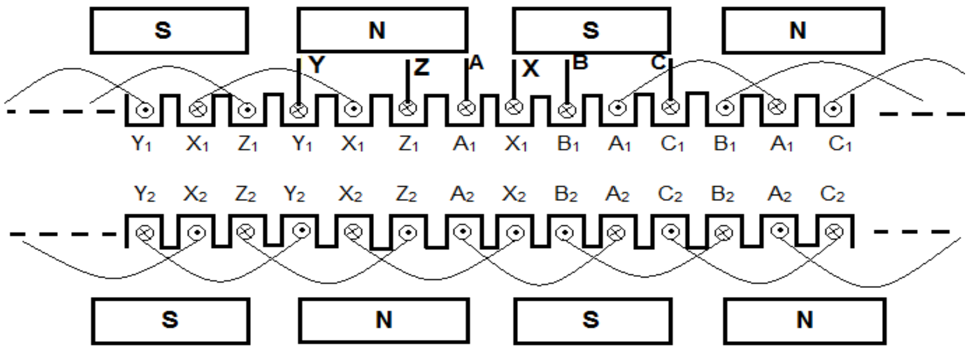

Figure 3 Axial flux PMSM electrical diagram

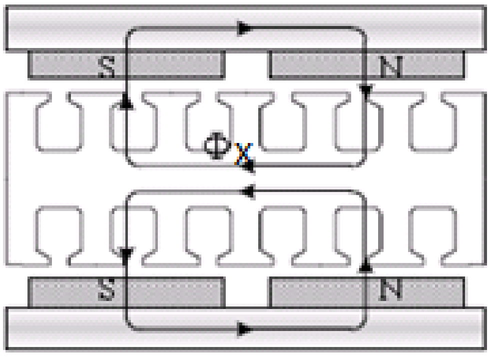

Figure 4 Interaction between the rotor and the stator

3. PROPOSED METHOD FOR ELECTROMOTIVE FORCES DETERMINATION

In this section, a method for computing the *EMFs* is proposed in order to model the dynamics of the *PMSM*. A road map for such modeling is presented in Fig. 5, and an equivalent internal circuit is shown in Fig. 6. In Fig. 5, the EMFs generated by the rotor magnets are calculated first, the parameters of the stator windings are found too, the interaction between the rotor and the stator are deduced in order to measure the stator voltages and currents upon a load connection. In Fig. 6, the equivalent internal circuit of a 6-phase PMSM is drawn in order to construct the model in Matlab/Simulink.

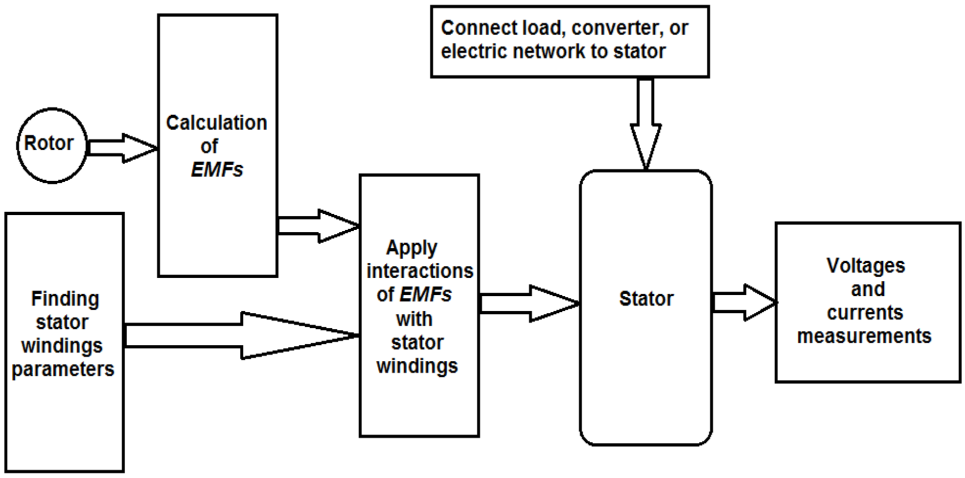

Figure 5 Road map for PMSM modeling

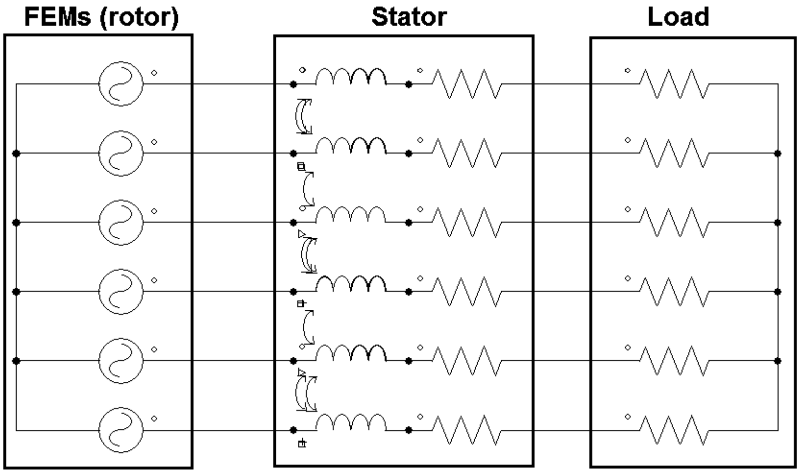

Figure 6 Equivalent internal circuit of the PMSM

The magnetic field for a certain point in the air gap is alternative trapezoidal in function of the angle of rotation. The trapezoidal shape can be decomposed in Fourier series where the fundamental of the magnetic field is first selected. Then, the harmonics may be added for more accuracy. Since we have 32 magnets disposed in a round over 360 degrees, the angle between two adjacent magnets N and S is 11.25 degrees. The general form of the magnetic field for a certain point in the airgap is deduced: $B(wt) = B_o \cos 16wt$, where B_o has to be determined from the parameters of the rotor magnets.

Since we have a symmetry of the magnets distribution for both sides of the coil in the stator, the fluxes of magnets adjacent to the one in face of the coil will cancel each other and sum to zero.

Then, the flux induced by the double rotor magnet in a coil of the phase 'a' on the stator (selected as reference) is $2.x.N.S.B_o.\cos 16wt$, where S is the area of the coil, N is the number of turns of the coil, B_o is the intensity of the magnetic field created by a single magnet, and x is a constant and represents the fraction of the flux linkage (coupled with the stator windings) of the rotor magnet to the total flux (denoted Φx in Fig. 4).

As explained in the previous section, the disposition between the magnet and a pole in a phase is the same for all poles in the same phase.

The coils of the poles are connected in series, so: the flux induced in the phase 'a' is:

$$\lambda_{ra} = 32xNSB_0 \cos 16wt \tag{1}$$

since we have 16 coils connected in series per phase.

The flux induced in phase 'b' is given by:

$$\lambda_{rb} = 32xNSB_0 \cos(16wt - x_b) \tag{2}$$

After a rotation of 7.5 degrees, the flux in the phase 'b' should be at its maximum, then: x_b = 120 degrees.

In a same manner, and for a symmetrical six-phase machine, the flux induced in the stator coils a, b, c, x, y, and z are:

$$\begin{bmatrix} \lambda_{ra} \\ \lambda_{rx} \\ \lambda_{rb} \\ \lambda_{ry} \\ \lambda_{rc} \\ \lambda_{rz} \end{bmatrix} = \begin{bmatrix} 32.x.B_o.N.S.\cos(16wt) \\ 32.x.B_o.N.S.\cos(16wt - \frac{\pi}{3}) \\ 32.x.B_o.N.S.\cos(16wt - \frac{2\pi}{3}) \\ 32.x.B_o.N.S.\cos(16wt - \pi) \\ 32.x.B_o.N.S.\cos(16wt + \frac{2\pi}{3}) \\ 32.x.B_o.N.S.\cos(16wt + \frac{\pi}{3}) \end{bmatrix} \tag{3}$$

Since the *emf* is the derivative of the created flux, we deduce:

$$\begin{bmatrix} EMF_a \\ EMF_x \\ EMF_b \\ EMF_y \\ EMF_c \\ EMF_z \end{bmatrix} = \begin{bmatrix} -512.w.x.B_o.N.S.\sin(16wt) \\ -512.w.x.B_o.N.S.\sin(16wt - \frac{\pi}{3}) \\ -512.w.x.B_o.N.S.\sin(16wt - \frac{2\pi}{3}) \\ -512.w.x.B_o.N.S.\sin(16wt - \pi) \\ -512.w.x.B_o.N.S.\sin(16wt + \frac{2\pi}{3}) \\ -512.w.x.B_o.N.S.\sin(16wt + \frac{\pi}{3}) \end{bmatrix} \tag{4}$$

The *emf*s when adding all the harmonics can be deduced:

$$\begin{bmatrix} EMF_a \\ EMF_x \\ EMF_b \\ EMF_y \\ EMF_c \\ EMF_z \end{bmatrix} = \begin{bmatrix} -\sum 512.k.h_k.w.x.B_o.N.S.\sin(16kwt) \\ -\sum 512.k.h_k.w.x.B_o.N.S.\sin(16kwt - \frac{\pi}{3}) \\ -\sum 512.k.h_k.w.x.B_o.N.S.\sin(16kwt - \frac{2\pi}{3}) \\ -\sum 512.k.h_k.w.x.B_o.N.S.\sin(16kwt - \pi) \\ -\sum 512.k.h_k.w.x.B_o.N.S.\sin(16kwt + \frac{2\pi}{3}) \\ -\sum 512.k.h_k.w.x.B_o.N.S.\sin(16kwt + \frac{\pi}{3}) \end{bmatrix} \tag{5}$$

Fig. 7 represents the shape of the magnetic field created by the rotor magnets in the air gap, whereas Fig. 8 represents the form of the EMFs generated according to the rotor position.

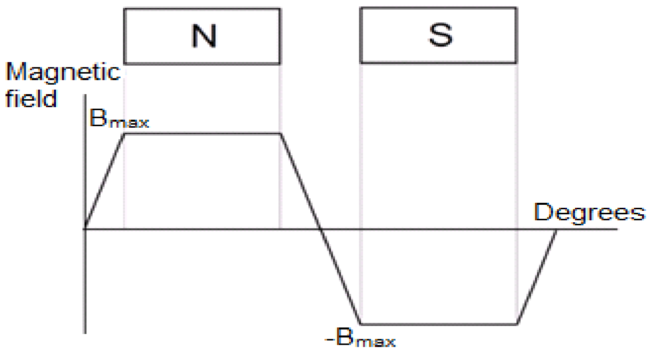

Figure 7 Shape of the magnetic field as a function of the magnet pole

In addition, the magnets distribution on the machine rotor are as following:
Pole step angle: 11.25°

Magnet opening angle: 7.5°

Angular space between two adjacent magnets: 3.75°

Then, the trapezoidal shape of the generated *emf* according to the position is given in Fig 8 with:

$$\theta_1 = 1^\circ.875, \theta_2 = 9^\circ.375, \theta_3 = 11^\circ.25,$$
$$\theta_4 = 13^\circ.125, \theta_5 = 20^\circ.625, \theta_6 = 22^\circ.5$$

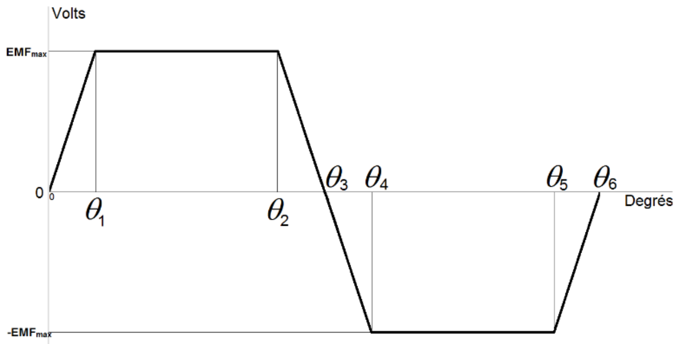

Figure 8 Curve of an EMF generated at 125 rpm

The magnitude h_k can then be determined from the Fourier analysis of the trapezoidal form.

Since the machine parameters are known (Appendix) except the term "x", the *emfs* magnitudes (fundamental and harmonics) in term of x are deduced as following:

Fundamental emf = 596.87x

Third harmonic emf = 132.64x

Fifth harmonic emf = 23.87x

Seventh harmonic emf = -12.18x

The most significant harmonics are chosen and integrated in the built model, the other harmonics magnitudes are neglected compared to the fundamental one.

4. DETERMINATION OF FLUX LINKAGE FRACTION

From the previous study and for a rotation speed of 125 rpm, the *emf* generated in phase "a" at no load operation can be expressed as:

$$emf = (-596.87\sin 16wt - 132.64\sin 48wt - 23.87\sin 80wt + 12.18\sin 112wt).x \quad (6)$$

By plotting this function (Fig. 9), we found that the peak value of this expression is

$$EMF_{max,\ theoretical} = 491x \quad (7)$$

The experimental machine emfs presented in Fig. 10 show a peak value of:

$$EMF_{max,\ experimental} = 108V \quad (8)$$

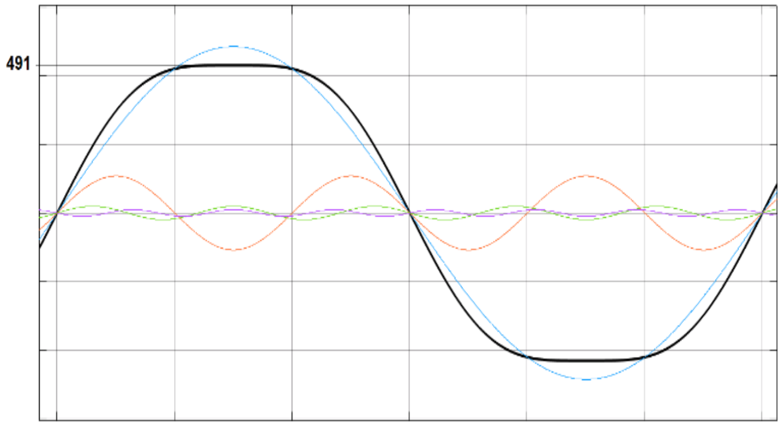

Figure 9 Plot of the theoretical EMF and its harmonics

Comparing the two values of (7) and (8), *"x"* is determined:

x = 22% (9)

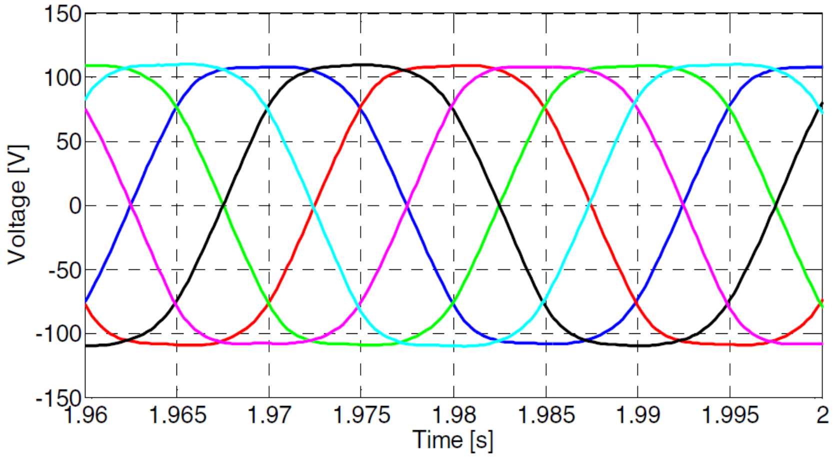

Figure 10 Experimental generated stator *emfs* at 125 rpm

5. WINDINGS PARAMETERS DETERMINATION

To determine the parameters of the machine stator windings, simple tests have been performed:

For the winding resistance, a DC voltage V is applied across a single phase at no rotor movement and the current I is measured. The resistance is determined by the formula in equation 10:

$$R_L = \frac{V}{I} \tag{10}$$

Noting a zero voltage across the inductive component of the winding in DC mode.

For the self-inductance determination, an AC voltage v is applied across the phase at no rotor movement and the current i is measured. The self-inductance is determined by the formula in equation 11 which leads to equation 12:

$$\dot{V} = \dot{I}(R + j\omega L) \tag{11}$$

$$L = \sqrt{\frac{v^2 - R_L^2 i^2}{\omega^2 i^2}} \tag{12}$$

For the mutual inductance between two phases “m” and “n”: an AC voltage v_m is applied across the phase “m” at no rotor movement, the current i_m in the phase “m” is measured, the voltage v_n across the phase “n” is measured at open circuit. The mutual inductance M_{mn} is determined by the formula in equation 13 which leads to equation 14:

$$\dot{V}_n = j\omega M_{mn} \dot{I}_m \tag{13}$$

$$M_{mn} = \frac{v_n}{\omega i_m} \tag{14}$$

The values are given in the appendix of this paper.

6. MODEL ASSESSMENT

The model has been built in the Matlab/Simulink environment. Fig. 11 shows the built model. A 12 ohms six-phase resistive load is connected on the machine stator terminals and the rotor was turned with a speed of 125 turn/min by a training motor fixed on the same rotor axis. The model has been tested with a six-phase resistive load equal to 12 ohms and compared to the experimental results. Fig. 13 depicts the electromotive forces obtained with the model simulation while the experimental results are given in the same conditions in Fig. 10.

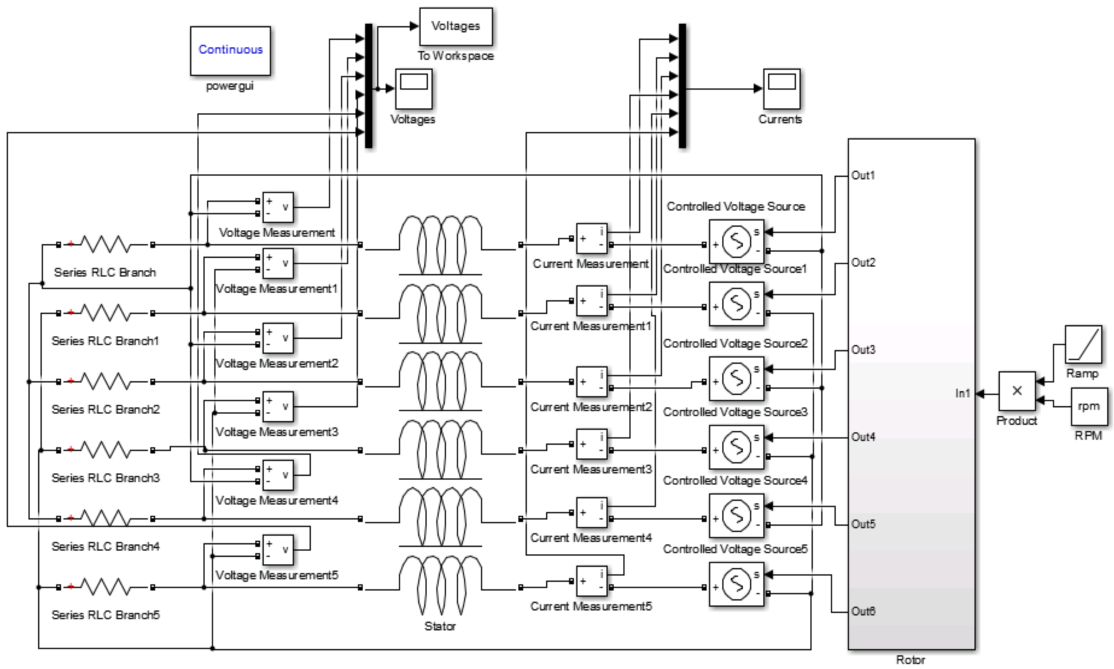

Figure 11 The model built in Matlab/Simulink

Several tests have been done to assure the accuracy of the model.

The experimentations have been realized using a test bed built in our laboratory as shown on Fig. 12. It is composed of a wind emulator which is realized with a classical three-phase induction machine (45kW-1500rpm) controlled by an industrial variable speed drive, and which is linked to a gearbox with a ratio of 11.2 in order to reduce the mechanical speed (0 to 133rpm). This will then drive the PMSM (24kW) to operate in generator mode. The speed is measured by a non-contact inductive sensor to ensure a precise angular measurement.

The PMSM is connected to the grid via a back-to-back converter of 15 kVA that is controlled by an industrial PC in real time using MATLAB-Simulink. The control and acquisition of the measured quantities is done with a switching frequency of 10 kHz.

Figure 12 Experimental test bed

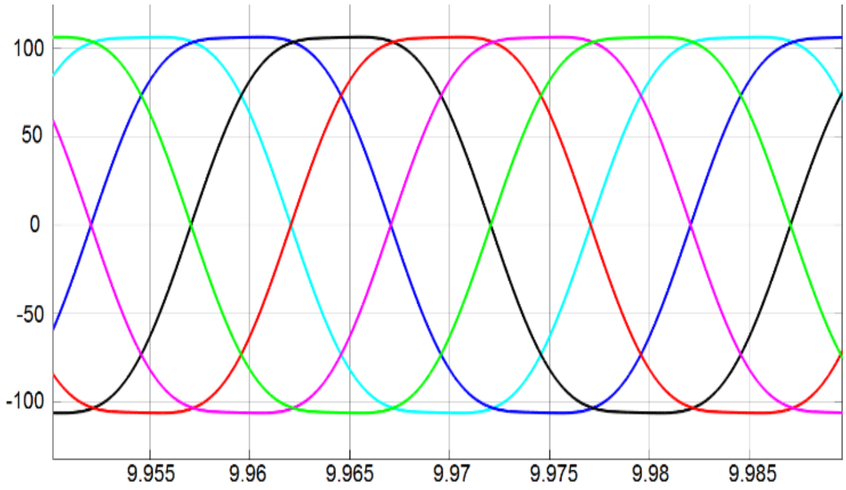

Figure 13 EMFs generated on the stator (model simulation)

The model has been tested also with a single open-phase fault with the speed of 125 turn/min also. Fig. 14 and Fig. 15 show the simulated and experimental results of the currents in the stator windings. By comparison, it is clearly shown that the simulation and the experimental results are really identical for all considered cases and the model is successfully validated.

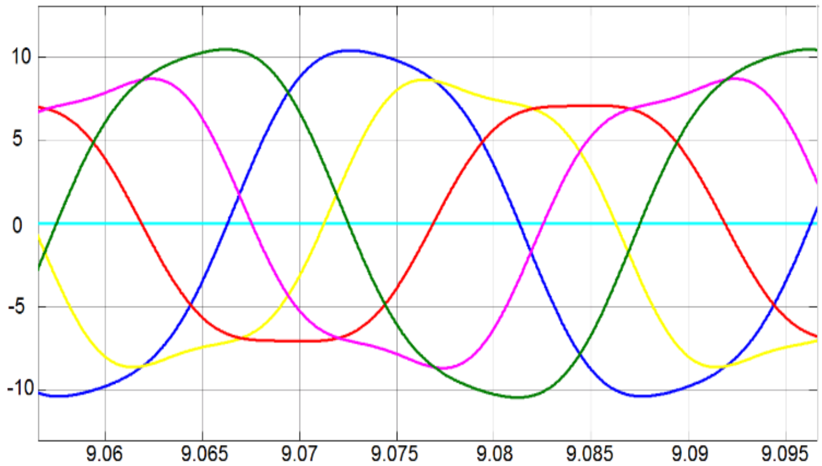

Figure 14 Currents in the stator for one open-phase (model simulation)

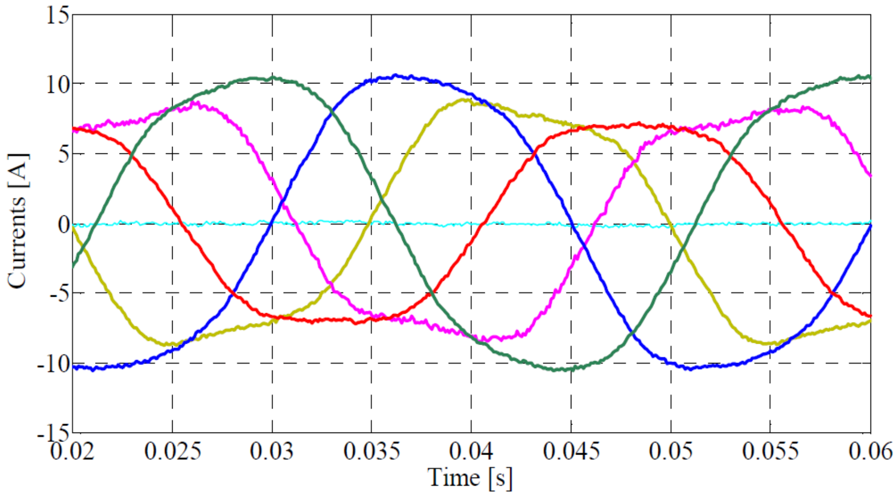

Figure 15 Currents in the stator for one open-phase (experimental)

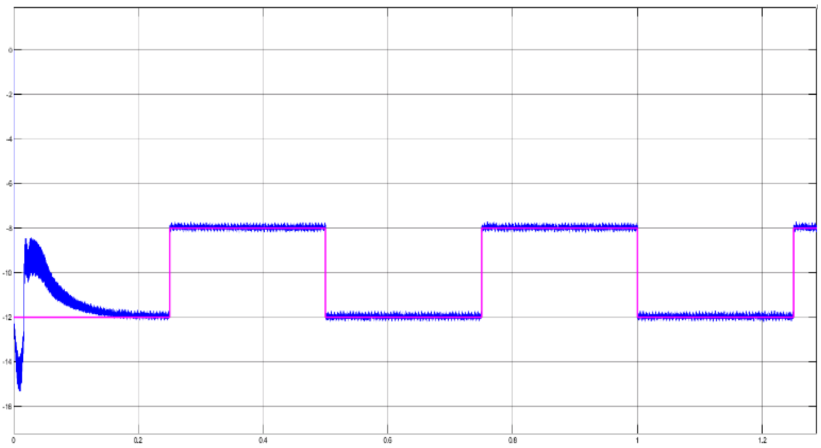

Figure 16 Simulation results of the reference and measured currents for “q” component

In addition, the model has been tested to extract the electrical energy generated by the machine (wind turbine application). Indeed, *PI* controllers associated to the field oriented control (FOC) strategy are used to regulate the currents generated by the machine and to follow references given by their “d” and “q” components. Fig. 16 shows the simulation results of the reference and measured currents for the “q” component which demonstrate clearly that the reference current is well tracked, keeping on zero “d” component.

7. CONCLUSION

In this work, a simple model for a six-phase axial flux *PMSM* is designed and built using Matlab/Simulink software. The model has been tested for several topologies, namely with equilibrate load, with a single fault, and with an interface with grid. A comparison between the simulated and experimental results has been performed in order to validate the model accuracy. Also, the model has been built by using the internal circuit oriented approach which allows a very accurate simulation of the machine dynamics. The future work consists of using this model in order to inject the electrical energy generated by the *PMSM* (wind turbine application) into the grid and propose a fault tolerant control which assure the continuity of the energy generation and injection for several faults topologies.

NOMENCLATURE

B_o: Intensity of the magnetic field created by a single magnet of the rotor,

λ_{ra}: Flux created by the rotor and induced in phase "a",

λ_{rb}: Flux created by the rotor and induced in phase "b",

EMF_n: Electromotive force generated in phase "n",

X: Fraction of the flux linkage (coupled with the stator windings) of the rotor magnet to the total flux,

ω: Speed of the rotor in rad/s,

S: Area of the coil in the stator windings,

N: Number of turns of the coil in the stator windings per pole in one phase,

R_L: Resistance of the stator winding per phase,

V: Voltage applied on a stator phase,

I: Current circulating in a stator phase,

L: Self inductance of stator winding per phase,

M_{mn}: Mutual inductance between phase "m" and phase "n".

APPENDIX

Table 1 6AFPMSM rated Parameters

Rated power	24 kW
Rated torque	1800 N.m
Rated current	47 A
Rated back-EMF	87V
Rated speed	125 rpm
Rated frequency	33 Hz
Constant K	0.67 V/rad/s

Table 2 6AFPMSM Geometrical Parameters

Poles	32
Number of stator phases	6
Turn of coil	17
Stator slots	96
Number of rotor magnets	32
Airgap	2 [mm]
Stator yoke	41 [mm]
Outer stator yoke radius	305 [mm]
Inner stator yoke radius	220 [mm]
Rotor yoke	20 [mm]
Outer rotor yoke radius	305 [mm]
Inner rotor yoke radius	125 [mm]

$N(turns) = 17$

$B_o(T) = 1.26$

Average $S(m^2) = 0.008528$

$$R_{ss}(\Omega) = \begin{bmatrix} 0.2 & 0 & 0 & 0 & 0 & 0 \\ 0 & 0.2 & 0 & 0 & 0 & 0 \\ 0 & 0 & 0.2 & 0 & 0 & 0 \\ 0 & 0 & 0 & 0.2 & 0 & 0 \\ 0 & 0 & 0 & 0 & 0.2 & 0 \\ 0 & 0 & 0 & 0 & 0 & 0.2 \end{bmatrix}$$

$$L_{ss}(H) = \begin{bmatrix} 0.002 & 0.0004 & -0.0002 & 0 & -0.0002 & 0.0004 \\ 0.0004 & 0.002 & 0.0004 & -0.0002 & 0 & -0.0002 \\ -0.0002 & 0.0004 & 0.002 & 0.0004 & -0.0002 & 0 \\ 0 & -0.0002 & 0.0004 & 0.002 & 0.0004 & -0.0002 \\ -0.0002 & 0 & -0.0002 & 0.0004 & 0.002 & 0.0004 \\ 0.0004 & -0.0002 & 0 & -0.0002 & 0.0004 & 0.002 \end{bmatrix}$$

REFERENCES

[1] Y. Demir and M. Aydin, "A Novel Dual Three-Phase Permanent Magnet Synchronous Motor with Asymmetric Stator Winding," in IEEE Transactions on Magnetics, vol. 52, no. 7, pp. 1-5, July 2016, Art no. 8105005.

[2] A. Matyas, G. Aroquiadassou, A. Mpanda-Mabwe, C. Martis and K. Biro, "Torque ripple analysis of a 42V fault tolerant six-phase permanent magnet synchronous machine," IECON 2010 - 36th Annual Conference on IEEE Industrial Electronics Society, Glendale, AZ, 2010, pp. 1011-1016.

[3] M. Salehifar, R. S. Arashloo, M. Moreno-Eguilaz and V. Sala, "Open circuit fault detection based on emerging FCS-MPC in power electronics systems," 2013 15th European Conference on Power Electronics and Applications (EPE), Lille, 2013, pp. 1-10.

[4] S. Dwari and L. Parsa, "An Optimal Control Technique for Multiphase PM Machines Under Open-Circuit Faults," in IEEE Transactions on Industrial Electronics, vol. 55, no. 5, pp. 1988-1995, May 2008.

[5] N. A. Karim, J. Azzouzi, G. Barakat and B. Dakyo, "Complete Analytical Modeling of an Axial Flux PM Synchronous Machine for Wind Energy Application," 2006 12th International Power Electronics and Motion Control Conference, Portoroz, 2006, pp. 996-1001.

[6] A. Egea, G. Almandoz, J. Poza and A. Gonzalez, "Analytic model of axial flux permanent magnet machines considering spatial harmonics," SPEEDAM 2010, Pisa, 2010, pp. 495-500.

[7] P. Wang, P. Zheng, Y. Sui, F. Wu, L. Cheng and T. Li, "Design and analytical inductance calculations of five-phase fault-tolerant permanent-magnet Machine," 2014 17th International Conference on Electrical Machines and Systems (ICEMS), Hangzhou, 2014, pp. 1639-1642.

[8] G.K. Singh, “Modeling and analysis of six-phase synchronous generator for stand-alone renewable energy generation”, Elsevier, Volume 36, Issue 9, September 2011, Pages 5621-5631.

[9] A. Pantea et al., "Six-Phase Induction Machine Model for Electrical Fault Simulation Using the Circuit-Oriented Method," in IEEE Transactions on Industrial Electronics, vol. 63, no. 1, pp. 494-503, Jan. 2016.

[10] A. Pantea, A. Yazidi, F. Betin, G. A. Capolino and V. Lanfranchi, "Six-phase Axial Flux Permanent Magnet generator model: Simulation and experimental validation," 2016 IEEE 25th International Symposium on Industrial Electronics (ISIE), Santa Clara, CA, 2016, pp. 192-197.